Remotely powered self-propelling particles and micropumps based on miniature diodes

SUK TAI CHANG[1], VESSELIN N. PAUNOV[2], DIMITER N. PETSEV[3] AND ORLIN D. VELEV[1]*

[1]Department of Chemical and Biomolecular Engineering, North Carolina State University, Raleigh, North Carolina 27695-7905, USA
[2]Surfactant & Colloid Group, Department of Chemistry, University of Hull, Hull HU6 7RX, UK
[3]Department of Chemical and Nuclear Engineering and Center for Biomedical Engineering, University of New Mexico, Albuquerque, New Mexico 87131, USA
*e-mail: odvelev@unity.ncsu.edu

Published online: 11 February 2007; doi:10.1038/nmat1843

Microsensors and micromachines that are capable of self-propulsion through fluids could revolutionize many aspects of technology. Few principles to propel such devices and supply them with energy are known. Here, we show that various types of miniature semiconductor diodes floating in water act as self-propelling particles when powered by an external alternating electric field. The millimetre-sized diodes rectify the voltage induced between their electrodes. The resulting particle-localized electro-osmotic flow propels them in the direction of either the cathode or the anode, depending on their surface charge. These rudimentary self-propelling devices can emit light or respond to light and could be controlled by internal logic. Diodes embedded in the walls of microfluidic channels provide locally distributed pumping or mixing functions powered by a global external field. The combined application of a.c. and d.c. fields in such devices allows decoupling of the velocity of the particles and the liquid and could be used for on-chip separations.

It is not easy to make small particles and devices that propel themselves in liquid. Viscous effects predominate on the microscale and render most mechanical means of propulsion inefficient[1–4]. The flagellar and ciliar bacterial motors are among the few natural chemical–mechanical ways of self-propulsion on the microscale[5–8]. Significant progress has been achieved in the synthesis of artificial molecular machines including molecular motors[9,10], shuttles[11] and 'nanocars'[12]. Such molecular machines can in principle propel microdevices or act as micropumps when attached to walls[13,14], but it is hard to adapt these complex natural or artificial molecular structures to engineered devices[15]. Two notable studies report bimetal-particle propulsion via catalytic decomposition of solutions of hydrogen peroxide[16,17]. Other papers discuss the undulatory motion of polymer gel under an electric field[18,19], a swimming screw machine driven by an external magnetic field[20], a camphor boat with ester vapour as a chemical stimulus[21], biomimetic swimming robots inspired by *Escherichia coli* motility[22], a carbon-fibre-based bioelectrochemical motor driven by the oxidation of glucose[23] and 'micro-oxen' cells moving microscale loads[24]. However, some of these particles only move in special media, whereas others cannot be scaled to microscopic dimensions.

Here, we demonstrate how various semiconductor diodes form a new class of self-propelling 'particles' and pumps in microfluidic devices. The energy is provided by a global external a.c. electric field. A d.c. voltage is induced between the electrodes of each diode as a result of rectification of the a.c. field. The constant electric field between the electrodes leads to electro-osmotic flow, which may propel the diodes or pump the adjacent liquid (Fig. 1). In effect, the semiconductor microelements harvest electric energy from external a.c. fields and convert it to mechanical propulsion on the microscale.

Two types of experiments were carried out to demonstrate how the flow of the adjacent liquid generated by the diodes can be used in microdevices. First, we studied how semiconductor diodes floating on the surface of water and aqueous solutions can self-propel directionally. The devices used included a range of regular (switching) diodes and diodes with additional functionality—light emitting diodes (LEDs), photodiodes and Zener diodes (for specifications, see the Supplementary Information). Their sizes ranged from 1 mm microdiodes to regular diodes of a few millimetres in length. The diodes floated suspended by the interfacial tension on the surface of water contained in a wide Petri dish. a.c. fields of square wave form, frequency 10 Hz–37 kHz and magnitude 30–150 V cm^{-1} were applied across the water by a pair of wire electrodes dipped at the sides of the container (Fig. 1).

The application of alternating electric fields did not lead to any perceptible liquid motion in the vessel or bubble formation at the thin wire electrodes. The field was spatially uniform and there were no dielectrophoretic forces[25–27] (other than torque) acting on the particles. The diodes suspended on the liquid surface first became oriented in the direction of the field lines (perpendicular to the electrodes) when the field was turned on. The microelements then began to move parallel to the electric field, always in only one direction with regards to the orientation of their anode and cathode (Fig. 2a,b). Velocities as high as millimetres per second were observed. Movies illustrating diode motion are provided in Supplementary Information, Movies M1–M3. The diodes were propelled with approximately constant velocity until reaching the opposite electrode and then stopped a few millimetres in front and above the electrode where the intensity of the field decreases. If the diodes were then rotated manually in the opposite direction, they moved with the same constant velocity until reaching the vicinity of the other electrode.

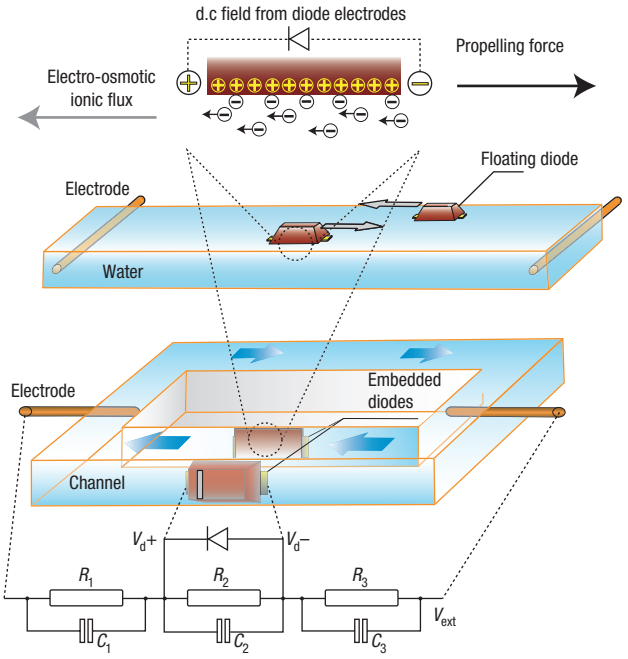

Figure 1 Schematic diagrams of the experiments for measuring floating-diode velocity and diode pumping rate in a model microfluidic device. The origin of the localized electro-osmotic flow and the equivalent electric circuit used to analyse the magnitude of the d.c. voltage, V_d, induced in the diode are shown in the top and bottom respectively.

We proved that the diode motility results from a local electro-osmotic flux powered by the external field. The specific direction of motion with regards to the diode cathode and anode indicates that a d.c. field along the diode is responsible for its mobility. The origin of this d.c. field can be understood by analysing the equivalent electric circuit of the experimental system, shown at the bottom of Fig. 1. The electric voltage induced in the diode by the external field can be estimated from a model including resistors describing the ionic conductance through the bulk liquid and capacitors for the ionic layers. At the low frequencies used in this study, the resistance is likely to be the leading contribution. The diode short-circuits the negative half-periods of the a.c. current. The resulting d.c. voltage of magnitude V_d induced in the diode can be approximated as

$$V_d = \frac{1}{2}\frac{R_2}{(R_1+R_2+R_3)}V_{ext}, \qquad (1)$$

where V_{ext} is the a.c. peak-to-peak voltage applied to the electrodes in the dish and R_1–R_3 are defined in Fig. 1. The coefficient of 1/2 accounts for the twofold decrease in the voltage during the rectification of a.c. into d.c. Assuming that the resistance of the liquid is linearly proportional to the distance between the electrodes, after expressing the external field intensity and substituting in equation (1), we arrive at the simple formula $V_d = E_{ext}l_d/2$, where l_d is the length of the diode body and E_{ext} is the external a.c. field. Commercial semiconductor diodes have an offset voltage in the forward direction, which is an intrinsic property of the pn junction[28]. In a real system, this offset voltage has to be compensated for by an additional field of E_{d0}. Thus, the above equation applied to real diodes reads:

$$V_d = \frac{l_d}{2}(E_{ext} - E_{d0}).$$

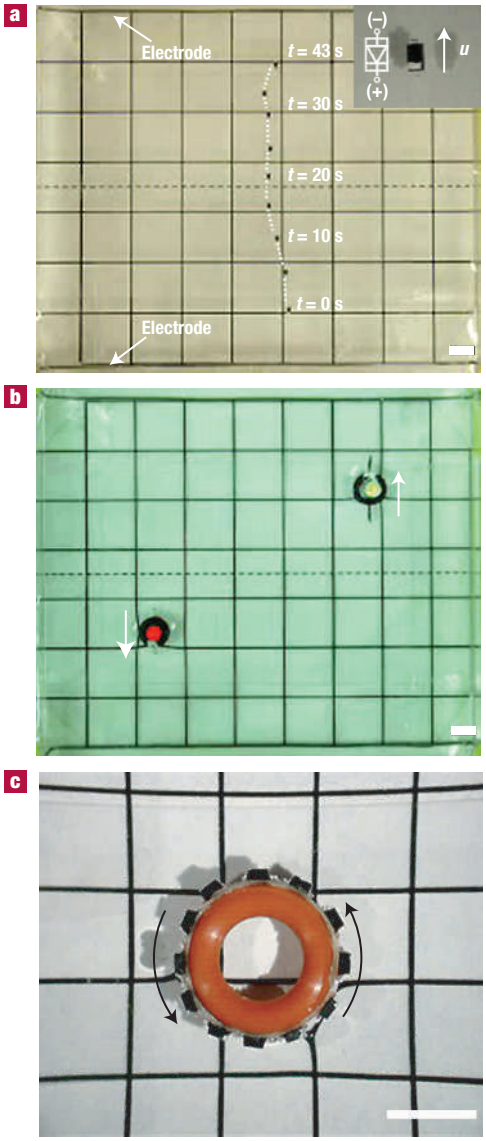

Figure 2 Optical micrographs of self-propelling semiconductor 'particles'. **a**, Overlay of a series of photographs at low magnification showing the 5 cm directional 'voyage' of a self-propelling microdiode (seen here as a small black rectangle) for a total duration of 43 s (see also Supplementary Information, Movie M2). **b**, Two LEDs light up and move towards the top or bottom depending on the orientation of their anodes (marked with white paint). This experiment demonstrates the potential of diode-based devices to deliver additional functionality on the basis of the voltage induced between their electrodes (see also Supplementary Information, Movie M3). **c**, The use of diodes as propellers and actuators in microelectromechanical systems —a rotor ring with diodes attached to its periphery spins around when an external field is applied (see also Supplementary Information, Movie M4). All experiments in **a**–**c** were carried out at external voltage $E_{ext} = 120\,V\,cm^{-1}$, frequency 1 kHz and 10^{-6} M NaCl. The scale bars represent 5 mm.

We measured the voltage generated across diodes dipped in the vessel as a function of the external field and distance between electrodes and found good quantitative agreement with this formula (see Supplementary Information, Fig. S1).

The d.c. field rectified between the electrodes gives rise to electro-osmotic fluid flow along the plastic body of the diodes.

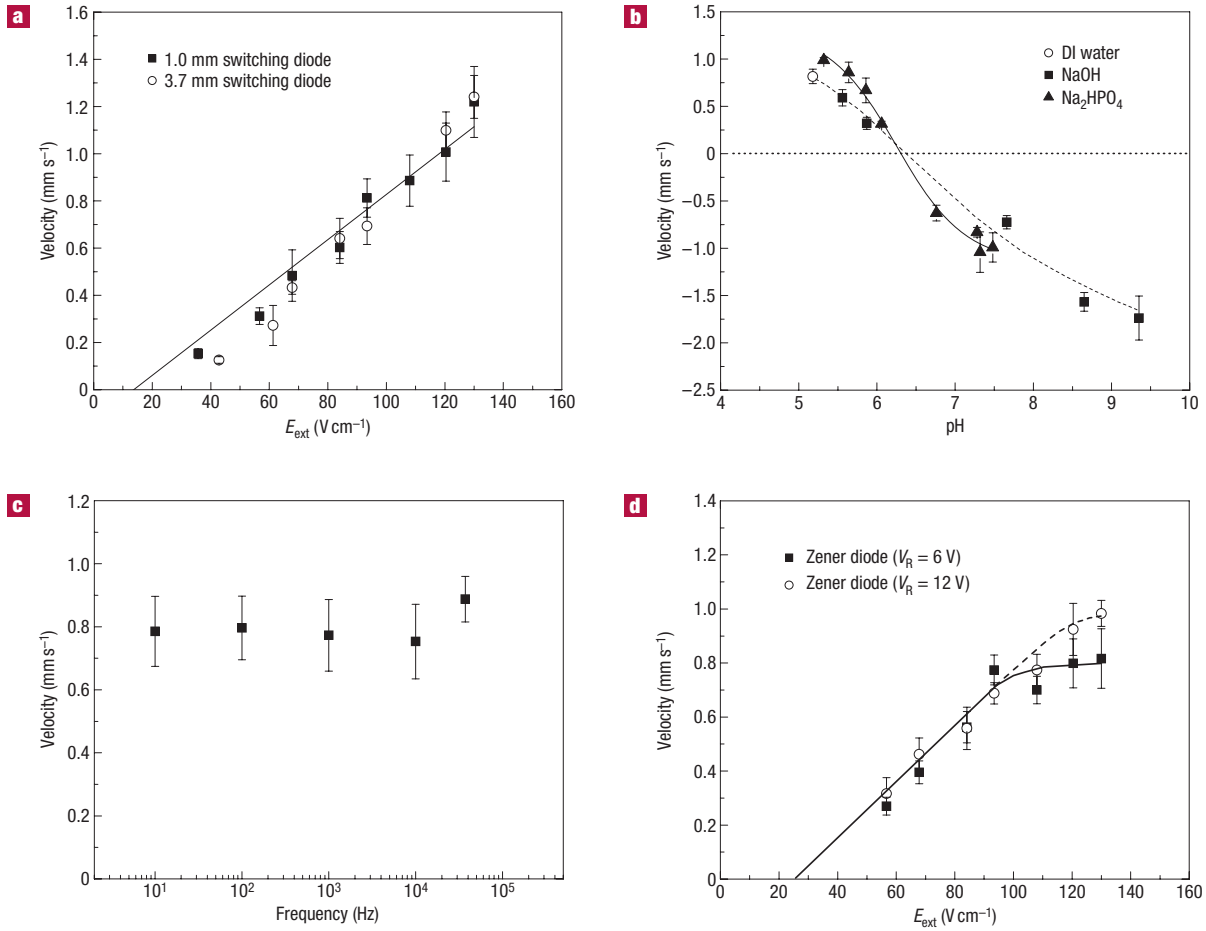

Figure 3 Dependence of the diode velocity on the parameters controlling the electro-osmotic propellant force. a, Velocity as a function of the external a.c. field. The line is plotted on the basis of equation (3) with only one fitting parameter, $\beta = 3.0$. Note that the velocities of the diodes are similar even though there is an almost fourfold difference in their size. **b**, Diode velocity as a function of pH. The direction of the motion changes at pH = 6.4, as the surface charge of the resin body changes sign at the isoelectric point. **c**, Diode velocity is not a function of the frequency of the external field up to frequencies in the RF region. **d**, When Zener diodes are used instead of switching diodes, the maximal velocity is restricted as a function of the characteristic reverse voltage of the Zener element. The curves are guides to the eye. Experiments **a**, **b** and **d** were carried out at 1 kHz. A 10^{-6} M NaCl solution was used in **a**, **c** and **d**. Experiments **b** and **c** were carried out at $E_{ext} = 93\,V\,cm^{-1}$. The error bars reflect the scatter in multiple experimental measurements.

This electro-osmotic effect is analogous to the one used to pump liquids in microfluidic devices[29,30], however, it originates here at an electronic device locally converting the energy of the external field into flow. The electro-osmotic flow reactively pushes the diodes in the opposite direction (see top portion of Fig. 1). The velocity of the electrokinetic flux, u_w, induced by the tangential d.c. field between the diode electrodes, E_w, can be estimated by the Helmholtz–Smoluchowski equation[31]

$$u_w = -\frac{\varepsilon\varepsilon_0\zeta}{\mu}E_w, \qquad (2)$$

where ε and ε_0 are the dielectric permittivity of the media and vacuum, respectively, μ is the viscosity of the liquid phase and ζ is the potential in the plane of hydrodynamic shear[31]. The velocity, u, of a particle floating on a free liquid interface is likely to be different to that of a completely submerged particle, so we add a hydrodynamic-resistance correction coefficient, β, to the equation: $u = -\beta u_w$. The electric field along the diode wall is $E_w = V_d/l_d$. Substituting these relations into equation (2), we obtain a formula estimating the diode velocity as a function of the intensity of the external a.c. field

$$u = \beta\frac{\varepsilon\varepsilon_0\zeta}{2\mu}(E_{ext} - E_{d0}). \qquad (3)$$

Notably, equations (2) and (3) differ not only in the coefficients, but in the type of electric field, d.c. in equation (2) and a.c. in equation (3). An intuitive way of presenting equation (3) is that a diode subjected to an external a.c. field will 'short-circuit' all half-periods of the field in the direction in which the diode is conductive; the remaining 'rectified' half-periods will generate electro-osmotic flux, which in turn will propel the diode. This formula demonstrates that the self-propelling effect reported here does not depend on the diode size, which cancels out from the expressions (provided that $E_{ext} \gg E_{d0}$ or that E_{d0} scales down with diode size). A microscopic diode-based device could move about as fast as a macrosized diode. We verified this simple model by experiments where the velocities of a 1 mm microdiode and a regular 3.7 mm diode were measured as a function of the applied

voltage (Fig. 3a). The velocities of both diodes were approximately equal (the average velocity of the microdiode was actually slightly higher at lower fields, possibly owing to the lower hydrodynamic drag). After substituting the value of E_{d0} measured experimentally in the static diode experiments, and assuming a typical value of $\zeta = 80\,\text{mV}$, we fitted these data by equation (3) with only one fitting parameter of $\beta = 3.0$. This is a reasonable value for the coefficient of hydrodynamic resistance, β, as the diode moves onto a free liquid surface and where the resistance is likely to be smaller than for a fully immersed particle. Verifying equation (3) for smaller diodes is currently difficult owing to the lack of commercial devices of such size. However, alternative fabrication techniques[32,33] might allow future testing of the technique with much smaller diodes and investigation of the effects of brownian motion and the counterionic atmosphere in the Hükel regime[31].

The electro-osmotic nature of the phenomena was proven by a variety of experiments. The ζ potential of the plastic diode surface is a function of pH, electrolyte concentration and the presence of charged surface-active species. We examined the effect of varying concentrations of acids, bases, charged surfactants and electrolytes on the diode mobility (Fig. 3b and Supplementary Information, Figs. S2,S3). The strongest effect is observed when the pH is increased by adding NaOH or Na_2HPO_4. The mobility of the diode first decreases and then changes direction (that is, instead of moving in the direction of their anode, the diodes begin to move with the cathode side in front). This can be attributed to recharging of the diode surface at higher pH. Indeed, when these data are plotted in coordinates of velocity versus pH (Fig. 3b), they overlap, indicating an isoelectric point of the diode polymer surface at pH ≈ 6.4. Negatively charged surfactant, sodium dodecyl sulphate, first suppressed the mobility of the diodes and then reversed their direction. Positively charged surfactant, cetyl trimethyl ammonium chloride, on the other hand, increased the diode mobility (see Supplementary Information, Fig. S2). Such effects are common in electro-osmosis and can be explained by a change in the intrinsic charge of the surface because of surfactant adsorption[31]. These changes in diode motion direction and velocity suggest a potential for sensing functions based on surface functionality. The effect of electrolyte was also typical for electro-osmotic-driven flows, as the velocity remained approximately constant at small electrolyte concentrations, whereas bubbling and electrochemical flows emerged at higher electrolyte concentrations (see Supplementary Information, Fig. S3). We also established that the diodes self-propel in non-aqueous media such as ethylene glycol and dimethyl sulphoxide (see Supplementary Information, Fig. S5).

Finally, we characterized the diode velocity in water as a function of the frequency of the external electric field (Fig. 3c). We found no correlation between these two parameters within the frequency range of 10 Hz–37 kHz. This result proves that the contribution of a.c. electrokinetic effects is negligibly small, as a.c. electrokinetics[25,34–40], arising from ionic mobility in electric field gradients, is strongly dependent on the field frequency. It also indicates that the diodes could be powered with fields in the radiofrequency (RF) or even microwave frequency range. Prototypes of small, inexpensive, yet complex, microcircuits powered remotely by external RF fields already exist in the form of radiofrequency identification microchips. Self-propelling diodes, powered remotely, may form the basis of a new class of microdevices of unprecedented complexity. We demonstrated rudimentary examples of a range of functionalities by using different types of commercial diodes (Table 1).

The voltage rectified between the diode electrodes can also be used to power additional functions of the electronic microcircuits. For example, LEDs suspended in the experimental vessel both propelled themselves electro-osmotically and emitted light (Fig. 2b, Supplementary Information, Movies M3,M5), demonstrating that the d.c. voltage rectified between the electrodes can power additional device functions. A rudimentary control of the velocity by a pre-programmed function of the semiconductor element was achieved using Zener diodes, which stabilize the reverse voltage on their pn junction at a certain threshold value[28]. Indeed, the electro-osmotic velocity of Zener diodes remained approximately constant above the corresponding value of the external voltage (Fig. 3d). Moving diodes can respond to external stimuli or signals, which was demonstrated by the use of photodiodes whose velocity could be controlled by light (see Supplementary Information, Fig. S4, Movie M6). The particle-localized electrohydrodynamic effect described here can also be used in diode-actuated electro-osmotic motors and actuators. This was illustrated by constructing 'gears' powered by a ring of regular switching diodes or by LEDs converting the energy of the external field into rotational motion (Fig. 2c and Supplementary Information, Movies M4,M5).

Table 1 Types of semiconductor elements used and functionality demonstrated.

Type of diode	Mobility specifics	Principle demonstrated
Regular switching	Moves with velocity $u \sim E_{ext}$	Electrohydrodynamic propulsion (Fig. 2a)
LED	Moves and emits light	Double functionality, propulsion and light emitting (Fig. 2b)
Zener	Moves at an approximately constant velocity above a certain E_{ext}	Internal electronic control of motility (Fig. 3d)
Photodiode	Movement stops when illuminated with a strong light source	External control of motility by light (see Supplementary Information, Fig. S4, Movie M6)

The electro-osmotic flux of the liquid generated between the diode electrodes can also be used to pump liquids on the microscale, if the diodes are immobilized. In the second cycle of experiments, we proved that the diodes can operate as distributed, locally operating, micropumps in microfluidic devices. The test microfluidic device constructed to evaluate the diode pumping action is schematically shown in the bottom half of Fig. 1. It was based on a closed rectangular channel 600 μm wide and 570 μm high and of overall dimensions of 20 mm × 5 mm. The a.c. field was applied to two electrodes situated symmetrically in the opposing short sections of the channel. Because of the symmetry of the channel and electrode placement, neither a.c. nor d.c. fields applied to the electrodes could engender macroscopic liquid circulation. The pumping was carried out by two diodes embedded in the opposing walls of the channel and oriented in the same direction. The liquid flow was observed using fluorescent tracer particles. When an a.c. field was applied to the electrodes, macroscopic circulation of the liquid around the channel was observed as a result of the local electro-osmotic flow driven by the diodes. At the same time, intense movement of the liquid in the direction of the macroscopic flow and a backflow in the middle of the channel were observed between the diode surfaces (Fig. 4a). The dependence of the microscopic velocity (measured in the channel without diodes) on the a.c. voltage applied (Fig. 4c) was similar to the velocity of diode propulsion (compare Figs 4c with 3a). Notably, these pumps operate at field intensities 20–100 times lower than the a.c. electrohydrodynamic pumps reported in the literature and do not need complex electrode micropatterns (a detailed comparison is presented in the Supplementary Information). Theoretical calculations of the macroscopic flux and computer simulations of the flow pattern in between the diodes were in excellent agreement

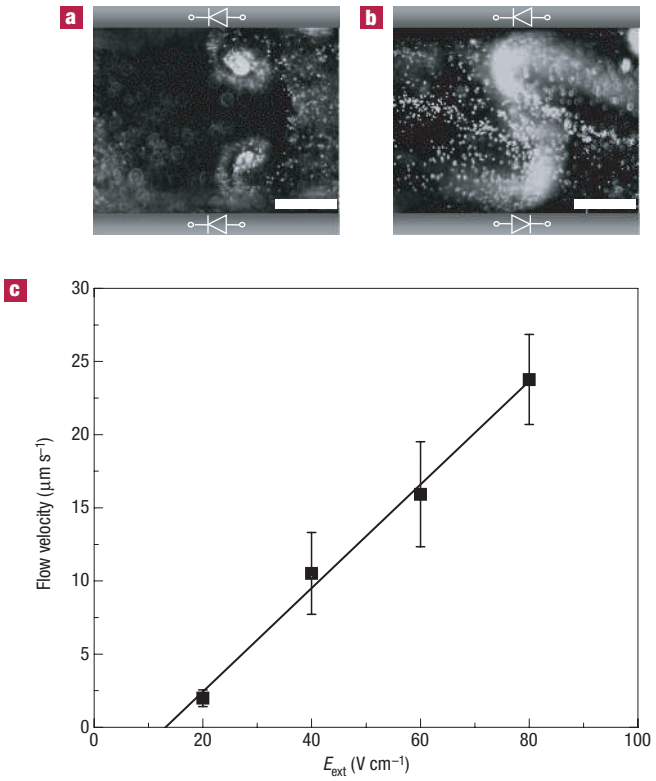

Figure 4 Flow of particle suspension in a microfluidic channel generated by two diodes embedded in the top and bottom sides of the channel, as observed from above. a, Optical micrograph illustrating pumping and backflow for diodes with the same orientation. The diodes create a unidirectional flow by moving the liquid adjacent to the wall in the same direction. **b**, Micrograph illustrating the flow generated by two diodes with opposite orientation. The diodes create a circular flow by moving the liquid adjacent to the wall in opposite directions, which can be used for microfluidic mixing. **c**, Velocity of the liquid pumped at the centre of the long channel without diodes (circulating through the microfluidic loop) as a function of the external a.c. field—compare with equation (3) and Fig. 3a. The error bars reflect the scatter in multiple experimental measurements. The scale bars represent 200 μm.

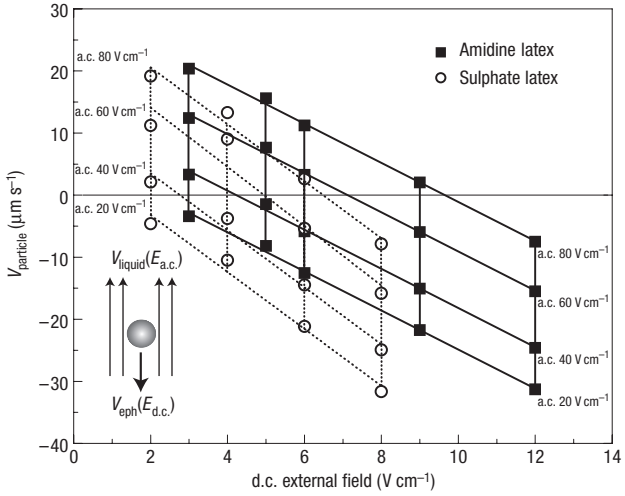

Figure 5 Particle velocities at the centre of the long channel without diodes as a function of the magnitude of the a.c. and d.c. components of the external field. The direction of the a.c. and d.c. driven effects is shown in the inset. The a.c.-driven diode pumps move the liquid in the positive direction. The increase in the d.c. component increases the (negative) electrophoretic velocity of the particles. At precisely adjusted values of the d.c. and a.c. fields near the position of dynamic equilibrium, particles with small differences in surface charge can be separated efficiently (see also Supplementary Information, Fig. S6 and Movie M7).

with the experimental data and will be published elsewhere. Instead of pumping the liquid, the two diodes in the channel wall could act as a microfluidic mixer when facing in opposite directions and creating a circular flow inside the channel (Fig. 4b).

A major advantage of this method is the ability to position multiple micropumps and mixers in different locations on the chip and power all of them with a global a.c. field (or RF waves) applied to the whole device. The a.c.-field-driven pumps open unique opportunities in microfluidics when combined with d.c. electrophoresis and d.c. electro-osmosis. One example is the ability to decouple the electrophoretic mobility of a particle or a biomolecule from the flow of the surrounding liquid. The difference in the charge and electrophoretic mobility is the major factor in the separation of proteins, polynucleotides, cells and particles in microfluidic devices[41–45]. The particles are separated in external d.c. field. Typically, however, the surrounding liquid also moves by electro-osmosis and particles with small differences in electrophoretic mobility might not be separated during the time they are transported through the channel[45]. The diode pumps, however, are actuated by a.c. fields, which do not affect the electrophoretic mobility of the particles outside the diode location. The velocity of a particle, $V_{particle}$, will be the sum of the electrophoretic, V_{eph}, and liquid, V_{liquid}, velocities

$$V_{particle} = V_{eph}(E_{d.c.}) + V_{liquid}(E_{a.c.}).$$

The d.c. and the a.c. components of the field can be applied simultaneously, but controlled independently. The a.c. field controls the liquid flow from the diode pump, whereas the d.c. field controls the electrophoretic particle velocity. If the a.c.-induced liquid flow is in a direction opposite to the one of the particles, they could be moved either in the positive direction, when $|V_{eph}| < |V_{liquid}|$, or in the negative direction, when $|V_{eph}| > |V_{liquid}|$. For each value of the d.c. component there is a value of the a.c. field where the electrophoretic mobility will be fully compensated by the diode-generated counterflux, so each type of particle in a mixture can be held in place by a dynamic equilibrium and separated from the others. By precisely adjusting the d.c. and a.c. components, particles with small differences in charge or size can be separated more efficiently than by electrophoresis alone. The ability to drive the diode pumps at the high frequencies and the relatively low fields used could avoid problems with fluid flows and vortices in areas of non-uniform field that may occur in pumping by conventional a.c. electrohydrodynamics[36–40].

We proved the above separation concept through experiments with a mixture of two types of negatively charged particles. The velocities of each particle type in the long channel (without the diodes) as a function of the d.c. and a.c. components of the field are plotted in Fig. 5. The principle of the technique can be illustrated by considering, for example, the velocity of the two types of particles at d.c. $= 6\,V\,cm^{-1}$ and a.c. $= 60\,V\,cm^{-1}$ (Fig. 5). The two particles move in different directions, even though they carry charges of the same sign. This process is illustrated in Supplementary Information, Movie M7 and the trajectories and velocities of the two particles are plotted in Supplementary Information, Fig. S6. Such microfluidic processes conveniently

controlled by two electrical parameters can lead to highly precise particle, cell and biomolecule separations and characterizations on a chip.

We demonstrate that semiconductor elements (diodes in this study and more complex devices in the future) may not only be used in electric circuits, but might also serve as building blocks for new classes of functional materials and devices. In future implementations, the power to the self-propelling particles and distributed electro-osmotic pumps could be provided by a.c. electric fields of higher frequencies potentially spanning the radiofrequency and microwave regions. The d.c. voltage rectified across the diode electrodes can be used to power microcircuits encased in the microdevices. The electro-osmotic propellency, combined with internal logic functions, may be used in dynamically reconfigurable microfluidic chips, spatially evolving active microsensor networks, or possibly in future complex motile devices such as microbots for medical diagnostics and surgery.

METHODS

The experiments, except the diode 'gear' experiment, were carried out in a plastic Petri dish of dimensions 9 cm × 9 cm × 1.5 cm in depth. Two thin wire electrodes were submerged on the top and bottom of the vessel with a distance of 7 cm between the electrodes, providing uniform electric field across the liquid. The diode 'gear' experiments were carried out in a vessel of dimensions 8 cm × 4 cm × 1 cm in depth with a 3.5 cm gap between the thin wire electrodes. The signal to the electrodes was provided by an a.c. generator (FG-7002C, EZ Digital) and amplifier (PZD 700, Trek), and was monitored with an oscilloscope and a digital voltmeter. The smaller diodes were floated directly on the surface of water suspended by the interfacial tension. Small floaters made of silicon glue were attached to the side of the larger switching diodes. The diode positions were observed with an Olympus SZ61 stereomicroscope and recorded with an attached Sony DSC-V1 digital camera.

The microfluidic chips were fabricated from poly(dimethylsiloxane) (PDMS) using soft lithography. The rectangular channel master was fabricated from SU-8 photoresist (MicroChem) on a silicon wafer. Two silicon switching diodes were attached to the side wall of the master at the centre of the longer channel using a 500-μm-thick sticky rubber patch. The PDMS (Sylgard 184, Dow Corining) was cast on the master with the attached diodes and cured at 70 °C. The PDMS replica with the embedded diodes was irreversibly sealed to a PDMS film coated on the glass slide using air-plasma cleaner (Model PDC-32G, Harrick Plasma). The particles used in the microfluidic experiments included fluorescent 1 μm amidine-stabilized polystyrene latex (Interfacial Dynamics) and fluorescent 2 μm sulphate-stabilized polystyrene latex (Molecular Probes). The diode pumping was characterized with a dispersion of 0.002 wt% 2 μm fluorescent latex in deionized (DI) water at pH ∼ 5.04 also containing 10^{-4} wt% Tween-20 and 10^{-5} M NaCl. The dispersions for the decoupling experiments contained 0.0002 wt% of amidine- and sulphate-stabilized latex particles each in pH ∼ 7.0 DI water with 10^{-4} wt% Tween-20 and 10^{-5} M NaCl. The particle ζ potentials at this pH measured by electrophoretic light scattering were −72.7 mV and −131 mV respectively. The suspensions were injected into the channel through two syringe needles inserted in the short channel sections. The external a.c. and d.c. electric fields were applied through the needles using the generator in the d.c.-offset mode. The motion of the particles was monitored using an Olympus BX-61 microscope in the reflection and fluorescent mode.

Received 3 August 2006; accepted 10 January 2007; published 11 February 2007.

References

1. Purcell, E. M. Life at low Reynolds number. *Am. J. Phys.* **45**, 3–11 (1977).
2. Brody, J. P., Yager, P., Goldstein, R. E. & Austin, R. H. Biotechnology at low Reynolds numbers. *Biophys. J.* **71**, 3430–3441 (1996).
3. Shapere, A. & Wilczek, F. Self-propulsion at low Reynolds number. *Phys. Rev. Lett.* **58**, 2051–2054 (1987).
4. Becker, L. E., Koehler, S. A. & Stone, H. A. On self-propulsion of micro-machines at low Reynolds number: Purcell's three-link swimmer. *J. Fluid Mech.* **490**, 15–35 (2003).
5. Berg, H. C. & Anderson, R. A. Bacteria swim by rotating their flagellar filaments. *Nature* **245**, 380–382 (1973).
6. Blair, D. F. & Berg, H. C. Restoration of torque in defective flagellar motors. *Science* **242**, 1678–1681 (1988).
7. Samuel, A. D. T. & Berg, H. C. Fluctuation analysis of rotational speeds of the bacterial flagellar motor. *Proc. Natl Acad. Sci. USA* **92**, 3502–3506 (1995).
8. Nelson, P. C. *Biological Physics: Energy, Information, Life* Ch. 5 (Freeman, New York, 2004).
9. Hernández, J. V., Kay, E. R. & Leigh, D. A. A reversible synthetic rotary molecular motor. *Science* **306**, 1532–1537 (2004).
10. Kelly, T. R., De Silva, H. & Silva, R. A. Unidirectional rotary motion in a molecular system. *Nature* **401**, 150–152 (1999).
11. Brouwer, A. M. *et al.* Photoinduction of fast, reversible translational motion in a hydrogen-bonded molecular shuttle. *Science* **291**, 2124–2128 (2001).
12. Shirai, Y., Osgood, A. J., Zhao, Y., Kelly, K. F. & Tour, J. M. Directional control in thermally driven single-molecule nanocars. *Nano Lett.* **5**, 2330–2334 (2005).
13. Vicario, J. *et al.* Nanomotor rotates microscale objects. *Nature* **440**, 163 (2006).
14. Darnton, N., Turner, L., Breuer, K. & Berg, H. C. Moving fluid with bacterial carpets. *Biophys. J.* **86**, 1863–1870 (2004).
15. Requicha, A. A. G. Nanorobots, NEMS, and nanoassembly. *Proc. IEEE* **91**, 1922–1933 (2003).
16. Ismagilov, R. F., Schwartz, A., Bowden, N. & Whitesides, G. M. Autonomous movement and self-assembly. *Angew. Chem. Int. Edn* **41**, 652–654 (2002).
17. Paxton, W. F. *et al.* Catalytic nanomotors: autonomous movement of striped nanorods. *J. Am. Chem. Soc.* **126**, 13424–13431 (2004).
18. Osada, Y., Okuzaki, H. & Hori, H. A polymer gel with electrically driven motility. *Nature* **355**, 242–244 (1992).
19. Osada, Y. & Gong, J. P. Soft and wet materials: polymer gels. *Adv. Mater.* **10**, 827–837 (1998).
20. Ishiyama, K., Sendoh, M., Yamazaki, A. & Arai, K. I. Swimming micro-machine driven by magnetic torque. *Sensors Actuat. A* **91**, 141–144 (2001).
21. Nakata, S. & Matsuo, K. Characteristic self-motion of a camphor boat sensitive to ester vapor. *Langmuir* **21**, 982–984 (2005).
22. Behkam, B. & Sitti, M. *Proc. Int. Mech. Eng. Conf. R&D Exposition* (Anaheim, California, 2004).
23. Mano, N. & Heller, A. Bioelectrochemical propulsion. *J. Am. Chem. Soc.* **127**, 11574–11575 (2005).
24. Weibel, D. B. *et al.* Microoxen: Microorganisms to move microscale loads. *Proc. Natl Acad. Sci. USA* **102**, 11963–11967 (2005).
25. Morgan, H. & Green, N. G. *AC Electrokinetics: Colloids and Nanoparticles* (Research Studies Press, Hertfordshire, 2002).
26. Velev, O. D. in *Colloids and Colloid Assemblies* (ed. Caruso, F.) 437–460 (Wiley-VCH, Weinheim, 2003).
27. Evoy, S. *et al.* Dielectrophoretic assembly and integration of nanowire devices with functional CMOS operating circuitry. *Microelectron. Eng.* **75**, 31–42 (2004).
28. Streetman, B. G. *Solid State Electronic Devices* 3rd edn, Ch. 6 (Prentice Hall, New Jersey, 1990).
29. Paul, P. H., Arnold, D. W., Neyer, D. W. & Smith, K. B. *Proc. μ-TAS 2000* (Enschede, Netherlands, 2000).
30. Chen, L. X., Ma, J. P., Tan, F. & Guan, Y. F. Generating high-pressure sub-microliter flow rate in packed microchannel by electroosmotic force: potential application in microfluidic systems. *Sensors Actuat. B* **88**, 260–265 (2003).
31. Hunter, R. J. *Foundations of Colloid Science* Ch. 8 (Oxford Univ. Press, New York, 2001).
32. Kovtyukhova, N. I. *et al.* Layer-by-layer assembly of rectifying junctions in and on metal nanowires. *J. Phys. Chem. B* **105**, 8762–8769 (2001).
33. Kovtyukhova, N. I. & Mallouk, T. E. Nanowire p-n heterojunction diodes made by templated assembly of multilayer carbon-nanotube/polymer/semiconductor-particle shells around metal nanowires. *Adv. Mater.* **17**, 187–192 (2005).
34. Ramos, A., Morgan, H., Green, N. G. & Castellanos, A. AC electrokinetics: a review of forces in microelectrode structures. *J. Phys. D: Appl. Phys.* **31**, 2338–2353 (1998).
35. Bhatt, K. H., Grego, S. & Velev, O. D. An AC electrokinetic technique for collection and concentration of particles and cells on patterned electrodes. *Langmuir* **21**, 6603–6612 (2005).
36. Dukhin, S. S. & Mishchuk, N. A. Concentration polarization of a conducting particle in strong fields. *Kolloidn. Zh.* **52**, 452–456 (1990).
37. Ajdari, A. Pumping liquids using asymmetric electrode arrays. *Phys. Rev. E* **61**, R45–R48 (2000).
38. Bazant, M. Z. & Squires, T. M. Induced-charge electrokinetic phenomena: Theory and microfluidic applications. *Phys. Rev. Lett.* **92**, 066101 (2004).
39. Debesset, S., Hayden, C. J., Dalton, C., Eijkel, J. C. T. & Manz, A. An AC electroosmotic micropump for circular chromatographic applications. *Lab Chip* **4**, 396–400 (2004).
40. Bazant, M. Z. & Ben, Y. Theoretical prediction of fast 3D AC electro-osmotic pumps. *Lab Chip* **6**, 1455–1461 (2006).
41. Greenlee, R. D. & Ivory, C. F. Protein focusing in a conductivity gradient. *Biotechnol. Prog.* **14**, 300–319 (1998).
42. Wang, Q., Lin, S. L., Warnick, K., Tolley, H. D. & Lee, M. Voltage-controlled separation of proteins by electromobility focusing in dialysis hollow fiber. *J. Chromatogr. A* **985**, 455–462 (2003).
43. Kaniaski, D. *et al.* Electrophoretic separations on chips with hydrodynamically closed separation systems. *Electrophoresis* **24**, 2208–2227 (2003).
44. Guttman, A. in *Electrokinetic Phenomena* (eds Rathore, A. S. & Guttman, A.) 69–108 (Marcel Dekker, New York, 2004).
45. Heiger, D. *High Performance Capillary Electrophoresis: An Introduction* (Agilent Technologies, Germany, 2000).

Acknowledgements

We acknowledge the Defense Advanced Research Projects Agency (DARPA/AFSOR) and NSF-CAREER (NCSU), NSF/NIRT and NSF/PREM DMR (UNM) and the EPSCR (UK) for support of this study. Correspondence and requests for materials should be addressed to O.D.V.
Supplementary Information accompanies this paper on www.nature.com/naturematerials.

Competing financial interests

The authors declare that they have no competing financial interests.